



# Statistical Analysis and Modeling of the Local Ionospheric Critical Frequency: A Mid-latitude Single-Station Model for Use in Forecasting

Danislav SAPUNDJIEV and Stanimir M. STANKOV

Royal Meteorological Institute of Belgium, Brussels, Belgium  
e-mail: danislav.sapundjiev@meteo.be

## Abstract

The hourly values of the  $F$ -layer critical frequency from the ionospheric sounder in Dourbes (50.1°N, 4.6°E) during the time interval from 1957 to 2010, comprising five solar cycles, were analyzed for the effects of the solar activity. The hourly time series were reduced to hourly monthly medians which in turn were used for fitting a single station  $f_oF_2$  monthly median model. Two functional approaches have been investigated: a statistical approach and a spectral approach. The solar flux  $F_{10.7}$  is used to model the dependence of  $f_oF_2$  on the solar activity and is incorporated into both models by a polynomial expression. The statistical model employs polynomial functions to fit the  $F$ -layer critical frequency while the spectral model is based on spectral decomposition of the measured data and offers a better physical interpretation of the fitting parameters. The daytime and nighttime  $f_oF_2$  values calculated by both approaches are compared during high and low solar activity. In general, the statistical model has a slightly lower uncertainty at the expense of the larger number of fitting parameters. However, the spectral approach is superior for modeling the periodic effects and performs better when comparing the results for high and low solar activity. Comparison with the International Reference Ionosphere (IRI 2012) shows that both local

models are better at describing the local values of the  $F$ -layer critical frequency.

**Key words:** ionosphere,  $F$ -layer critical frequency, monthly median.

## 1. INTRODUCTION

An operational system for local ionospheric nowcast and forecast is being developed to aid the monitoring of the ionospheric effects on the Global Navigation Satellite System (GNSS) applications (Stankov *et al.* 2012). In the forecast procedure, the ionospheric behavior is considered as composed of a periodic component (representing the average, non-disturbed conditions) and a random component (describing the disturbed, storm-time conditions). For the purpose of obtaining the periodic component with highest possible accuracy, an empirical model of the ionospheric critical frequency ( $foF_2$ ) is needed.

We have opted for a single-station model due to the following reasons: the global models tend to smooth out ionospheric features that are typical for a particular location and, therefore, a single-station model would yield better accuracy for use in local modeling, nowcast and forecast; it would be much easier to update the coefficients/statistical parameters of the model when new measurement data are incorporated; such a model would offer possibilities for a direct application in regional (such as over Europe) ionospheric mapping.

The ionospheric modeling at single stations has been of interest to the ionospheric community for some time already (Moraitis *et al.* 1991), leading to the development of several approaches and their implementation for ionospheric mapping and prediction. For example, in Europe, Stanisławska (1994) proposed an autocovariance prediction in which the predicted value (for instance  $foF_2$ ) is calculated in such a way that the covariance remains unchanged in the sense of the “minimum least squares” criterion. An advantage of this approach is that it requires only the existence of (sufficiently) long time series of observations of the modeled parameter – the nature of (geo-)physical processes and conditions governing the variations of this parameter may not necessarily be known and may not be (explicitly) used. Pancheva and Mukhtarov (1996) developed a spectral model of the  $foF_2$  monthly medians, describing the most important features of the diurnal, seasonal, and solar cycle variations of  $foF_2$ . An important distinction of this model from the model of Stanisławska (1994) is that it follows the natural sequence of the modulating mechanisms and, also, the solar activity is marked by two parameters – one for the activity level and one for the activity trend. Shortly after, a geomagnetically correlated statistical model (GCSM) was developed, incorporating the auto- and cross-correlation between the ionospheric char-

acteristic of interest and the geomagnetic index  $A_p$  (Muharov and Kutiev 1998). Liu *et al.* (2004) worked on single-station models based on Fourier expansion and cubic-B splines, and in doing so, investigated thoroughly the statistical relationship between  $foF_2$  and the solar proxies. Xu *et al.* (2008) used Fourier expansion to develop a single station spectral model of  $foF_2$  and to investigate the dependence of the local monthly median  $foF_2$  on solar activity and geomagnetic activity.

During the years, regional and global climatological models of  $foF_2$  were developed as well. For example, Fox and McNamara (1988) produced monthly median maps of  $foF_2$  based on worldwide ionosonde data and the Jones–Galley technique, for each hour, each month, and for high and low levels of solar activity. Based on Fourier analysis of ionospheric characteristics, Zolesi *et al.* (1993) developed a simplified ionospheric regional model (SIRM) for the European region. Mikhailov *et al.* (1996) offered another regional monthly median  $foF_2$  model (MQMF2) using the multiquadric functions for spatial interpolation. Monthly medians of the ionospheric characteristics are also offered by the International Reference model (IRI) (Bilitza 2001, IRI 2012). The ionospheric modeling and (instantaneous) mapping techniques evolved to consider solar and geomagnetic drivers as well (Muharov *et al.* 2001 and the references therein). As a result, more sophisticated tools and services for forecasting, nowcasting and warning of ionospheric propagation conditions were developed (Stamper *et al.* 2004).

The aim of this work is to create and evaluate a monthly median single station  $foF_2$  model for the ionospheric sounding station in Dourbes, Belgium. To achieve this goal, two methods for fitting the measured values were selected: spectral decomposition and polynomial functions. These methods were compared and evaluated by the deviations from the measured data. Additionally, the calculated values were compared against the IRI.

The paper is organized as follows: the measurements used for the study are presented; the methodology is elaborated, including the data analysis and model development; the model is evaluated with ionosonde measurements and via comparison with IRI2012. In the conclusion, an outlook for further developments and possible applications are discussed.

## 2. DATA

The measurements needed for the model are all made at the Geophysical Center of the Royal Meteorological Institute of Belgium (RMI) situated in Dourbes (50.1°N, 4.6°E) (Jodogne and Stankov 2002, Stankov *et al.* 2012). This is a complex observational site incorporating several observatories – ionosphere sounding, atmospheric, geomagnetic, cosmic rays, GPS TEC, *etc.*, all connected with optical-fiber communication lines. The first (analogue) ionosonde (Digisonde Panoramique) was installed in 1957 (recorded

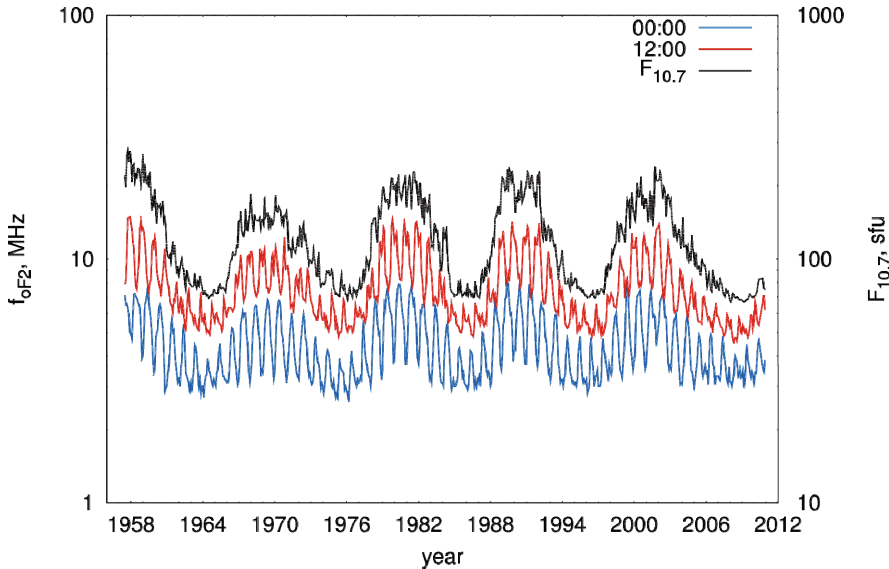


Fig. 1. Monthly median  $foF_2$  values measured at Dourbes at midnight (blue) and noon (red) together with the values of the  $F_{10.7}$  (black). The plot shows the periodic behavior of the hourly monthly median and its correlation to the solar activity index.

the ionograms on photographic films). The digital sounding started in September 1970 with a Digisonde-128, continued in 1984 with a Digisonde-256, and since April 2011 with a Digisonde-4D. All hourly values are manually verified until May 2012. The manually scaled data from this period was used to calculate the hourly monthly median values. The resulting values for the monthly median  $foF_2$  is plotted in Fig. 1 at 12:00 and 00:00 UTC.

### 3. METHODS DESCRIPTION

Modeling of the monthly median hourly values of the  $foF_2$  consists in solving the problem of time series analysis of periodic data for forecasting. The ultimate goal of this analysis is to find periodic patterns in the values and relate them to a process or the environment and to forecast future values based on available data of the environment or other pertinent parameters. In this work, the environmental parameter selected is the solar  $F_{10.7}$  index and we follow the standard methodology of time series analysis for data forecasting described by Montgomery *et al.* (2008).

#### 3.1 Data analysis

The monthly median values of the  $foF_2$  (Fig. 1) exhibit several periodic features with time and correlate strongly with the solar flux parameter,  $F_{10.7}$ .

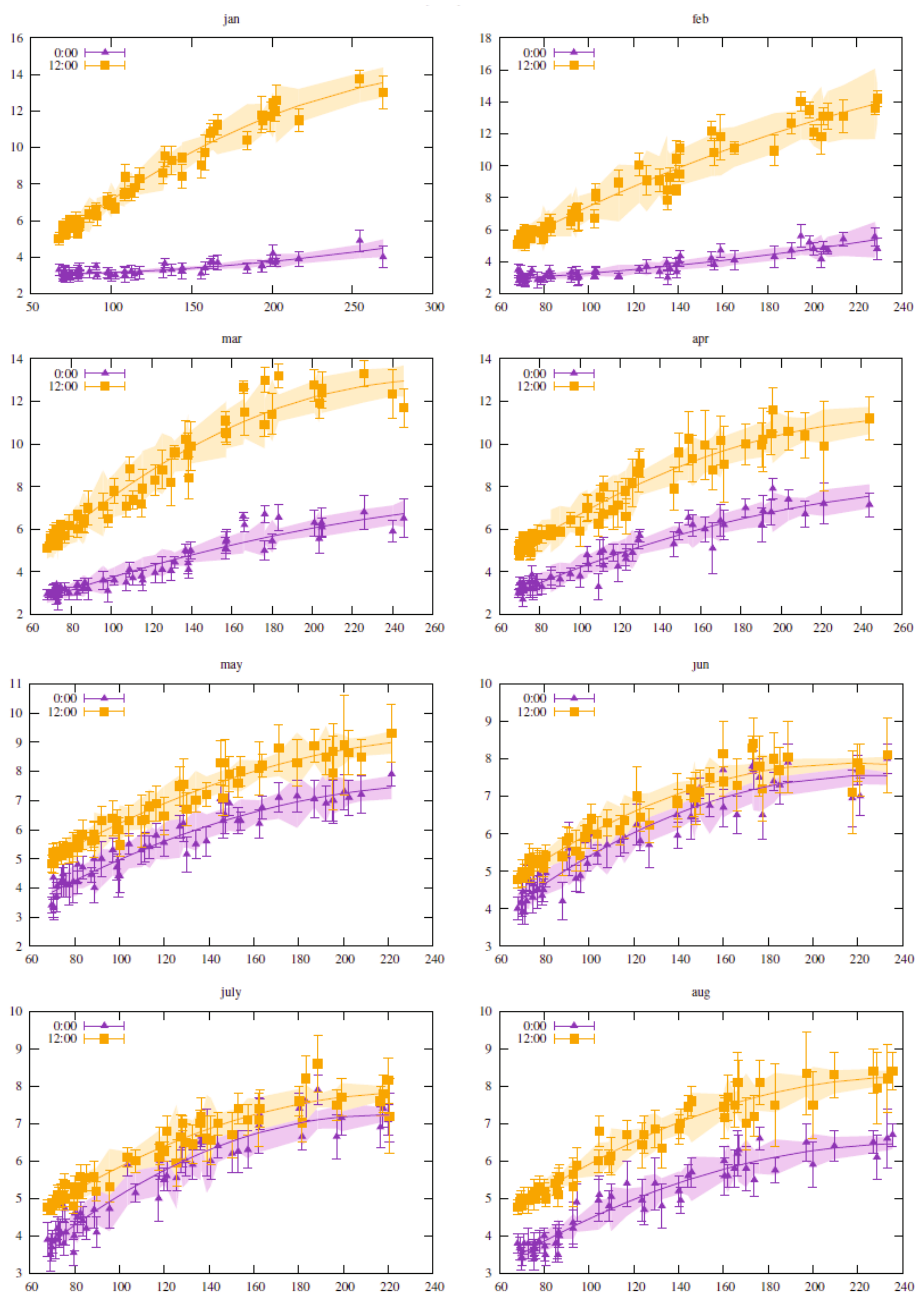


Fig. 2. Caption on next page.

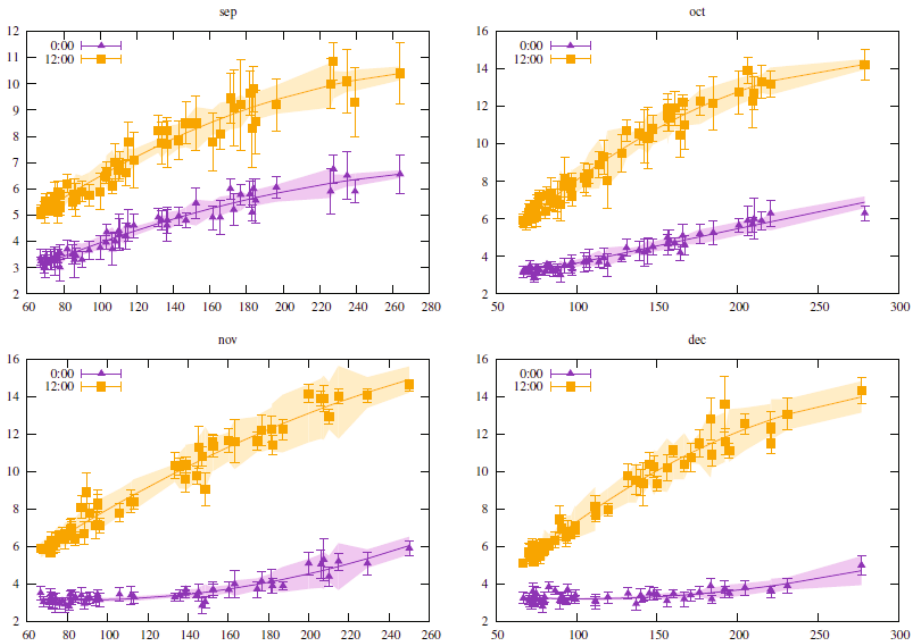


Fig. 2. The monthly median  $foF_2$  depends linearly or quadratically on the solar activity index  $F_{10.7}$  for each hour of the day and month of the year. The monthly median values at noon (12:00 UTC) and midnight (00:00 UTC) have been plotted against  $F_{10.7}$  for each month of the year, with the symbols denoting the measured values; the dotted lines are the fitting curves. The uncertainties of the modeled (fitted) values are given with the shaded areas.

Several periodic dependences can be identified from the plot of the monthly median  $foF_2$ : solar cycle, seasonal, and diurnal (Fig. 1). The periodic behavior suggests the use of a spectral decomposition to fit the measured values. There is another possible approach to model the  $foF_2$  which can be seen by plotting the latter against the solar activity parameter,  $F_{10.7}$  (Fig. 2) – the critical frequency at a given hour and month of the year depends linearly or quadratically on the solar flux parameter. This implies a simple method to model  $foF_2$  by fitting a polynomial function of the first or second degree to the data for each hour of the day and month of the year (Liu *et al.* 2004).

### 3.2 Methods implementation

The time dependent periodicities discussed in the previous section can be classified in two groups: indirect (*e.g.*, diurnal and seasonal) and direct, for instance, directly influenced by the solar activity. The indirect periodicities result from the rotation of the Earth and the orbiting. The solar cycle affects

the amplitudes of the diurnal and seasonal variations. A straightforward method to model the data is to decompose the diurnal and seasonal variations by fast Fourier transform, and to fit afterwards the amplitudes and the phases with a suitable polynomial to account for the solar cycle variations. This model is referred to as a spectral model and the approach has been used in the past for development and implementation of several single station models, *e.g.*, Zolesi *et al.* (1993), De Franceschi and De Santis (1994), Pancheva and Mukhtarov (1996), and Xu *et al.* (2008). The starting point of the spectral model is the Fourier transformation of the hourly monthly median values of the  $foF_2$ . For each  $F_{10.7}$  value, a Fourier transform of the  $foF_2$  is carried out without considering symmetry. The diurnal variation of the  $foF_2$  is then synthesized from the amplitude spectrum using the first 5 harmonics, as shown in Fig. 3, by the relation:

$$foF_2(m, F_{10.7}, t) = \sum_{i=0}^4 c_i(m, F_{10.7}) \cos[i2\pi/24t + \varphi_i(m, F_{10.7})], \quad (1)$$

where  $m$  is the month number (1-12),  $t$  is the time of the day,  $c_i$  and  $\varphi_i$  are the amplitude and the phase of the  $i$ -th harmonic in the Fourier decomposition.

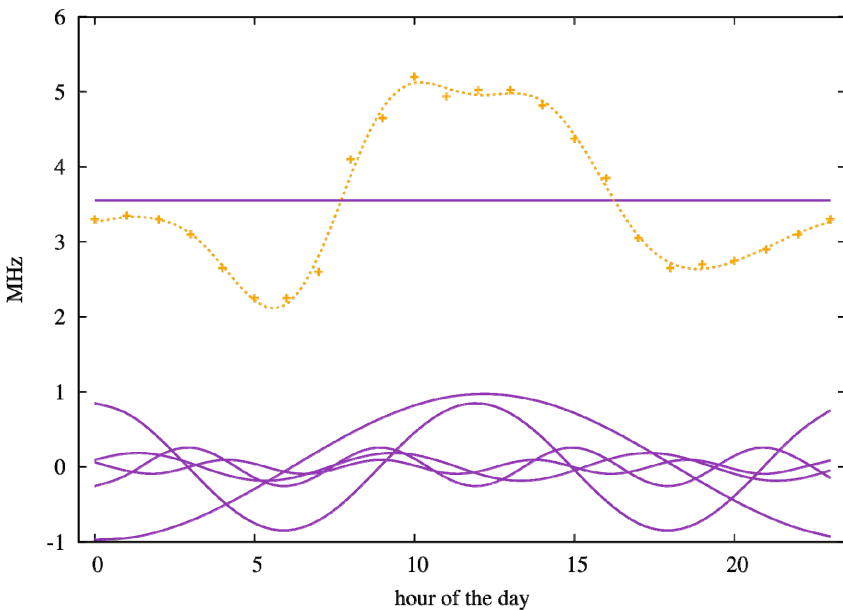


Fig. 3. Fourier decomposition of the daily variation (UT) of  $foF_2$  for January for  $F_{10.7} = 67.5$  sfu. The dashed line is the modeled diurnal variation; the crosses present the measured monthly median values and the solid lines – the harmonics used in the decomposition together with the constant component (the straight line).

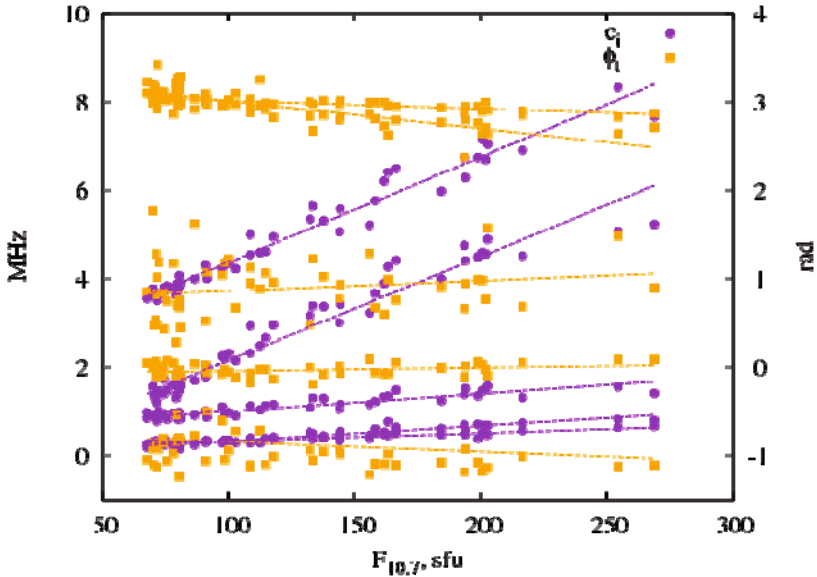


Fig. 4. Amplitudes,  $c_i$ , and phases,  $\varphi_i$ , of the Fourier transformation of the diurnal variation of  $foF_2$  (see Eqs. 1 and 2) versus the solar activity index  $F_{10.7}$ : the measured values (solid symbols) of the amplitudes are fitted (dashed lines) better by a second degree polynomial while for the phases a linear fitting function is sufficient.

The use of the few first harmonics is justified by their physical meaning and their stable dependence on the solar activity. Higher order harmonics are difficult to be physically interpreted and are not considered in this model. The amplitudes  $c_i(m, F_{10.7})$  and phases  $\varphi_i(m, F_{10.7})$ , as seen in Fig. 4, are easily modeled with a quadratic and a linear function of  $F_{10.7}$  for each hour of the day and the current month  $m$ . Thus, for the amplitudes and the phases we obtain:

$$c_i(m, F_{10.7}) = \sum_{j=0}^2 a_{ij}(m) F_{10.7}^j, \quad \varphi_i(m, F_{10.7}) = \sum_{j=0}^1 b_{ij}(m) F_{10.7}^j, \quad (2)$$

where  $i \in [0, 4]$  stands for the number of harmonics used for the spectral decomposition of  $foF_2$  and  $a_{ij}$  and  $b_{ij}$  are the fitting coefficients. With this representation,  $foF_2$  can be expressed as:

$$foF_2(m, F_{10.7}, t) = \sum_{i=0}^4 \sum_{j=0}^2 [a_{ij}(m) F_{10.7}^j] \cos \left[ i2\pi/24t + \sum_{j=0}^1 b_{ij}(m) F_{10.7}^j \right]. \quad (3)$$

The second temporal parameter is the monthly variation of the  $foF_2$ . This is expressed by another Fourier transformation of the fitting coefficients  $a_{ij}$  and  $b_{ij}$ :



$$\begin{aligned} a_{ij}(m) &= \sum_{k=0}^5 x_{ijk} \cos(k2\pi/12m + \chi_{ijk}), \\ b_{ij}(m) &= \sum_{k=0}^5 y_{ijk} \cos(k2\pi/12m + \psi_{ijk}), \end{aligned} \quad (4)$$

where the summation is over all 6 harmonics with amplitudes  $x_{ijk}$  and  $y_{ijk}$ , and phases  $\chi_{ijk}$  and  $\psi_{ijk}$ . Finally, the dependence on the solar activity has to be eliminated from the equations. In the above Fourier expressions, the dependence on the solar activity is contained within the parameters (amplitude and phases) of the decomposition, which are plotted in Fig. 4. The final expression for  $foF_2$  becomes:

$$\begin{aligned} foF_2(m, F_{10.7}, t) &= \sum_{i=0}^4 \left[ \sum_{j=0}^2 \left\{ \sum_{k=0}^5 \left[ x_{ijk} \cos(k2\pi/12m + \chi_{ijk}) \right] F_{10.7}^j \{ i2\pi/24t + \right. \right. \\ &\quad \left. \left. \sum_{j=0}^1 b_{ij}(m) F_{10.7}^j \sum_{k=0}^5 \left[ y_{ijk} \cos(k2\pi/12m + \psi_{ijk}) \right] F_{10.7}^j \right\} \right]. \end{aligned} \quad (5)$$

With this, the total number of parameters required to calculate the  $foF_2$  is 150 ( $5 \times 3 \times 6 + 5 \times 2 \times 6 = 150$ ).

Another approach to fit the monthly median dependence of  $foF_2$  is to use polynomials of various degrees, as proposed and implemented by *Liu et al.* (2004):

$$foF_2(h, m, F_{10.7}) = a_{mh} F_{10.7}^2 + b_{mh} F_{10.7} + c_{mh}, \quad (6)$$

where the indices  $m$  and  $h$  stand for month and hour and  $a$ ,  $b$ , and  $c$  are the fitting coefficients. This approach permits to calculate  $foF_2$  if we know  $F_{10.7}$  at an arbitrary date and hour. This approach is referred as the polynomial model in this work and as statistical model elsewhere (*Liu et al.* 2004). In total, this results in 3 coefficients per fitting for each month and for each hour, *i.e.*, 864 coefficients in total ( $3 \times 12 \times 24 = 864$ ). As we can see from the expression of the  $foF_2$ , the dependence on the time (hour and month) is described by the indices of the expansion. A limitation of this model is that it does not accept decimal values for the hour and the month, whereas the spectral model, see Eq. 5, allows the use of decimal time and month.

## 4. EVALUATION OF THE MODELS

### 4.1 Comparison with measurements

Using the approaches described in the previous section, the monthly median  $foF_2$  is calculated and plotted in Figs. 5 and 6 together with the measured monthly median values. For the uncertainty of the measured value, the

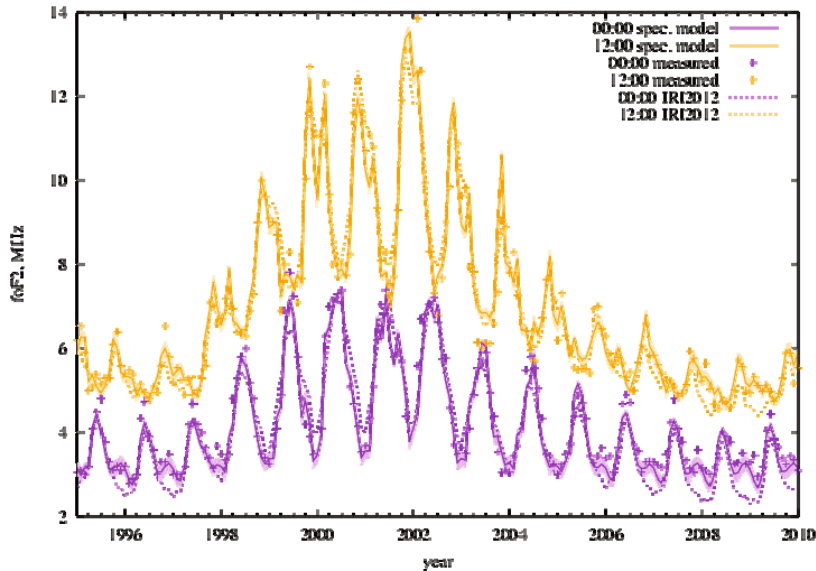


Fig. 5. Hourly monthly medians of  $foF_2$  for one solar cycle at noon and at midnight obtained by the polynomial fitting model (solid lines), together with the measured monthly median (plus sign), and the calculated values by IRI2012 (dashed lines). The uncertainties of the modelled values are given by the shaded lines.

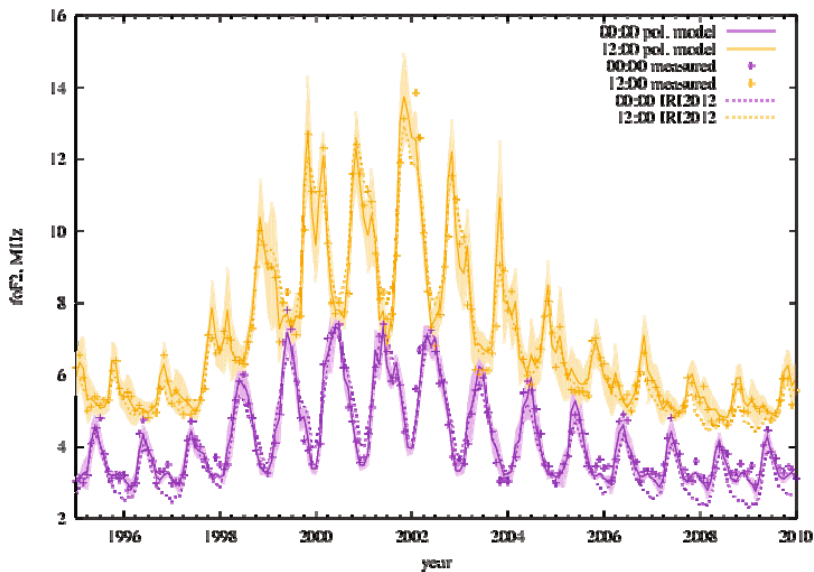


Fig. 6. Hourly monthly medians of  $foF_2$  for one solar cycle at noon and at midnight obtained by the spectral model (solid lines), together with the measured monthly median (plus sign), and the calculated values by IRI2012 (dashed lines). The uncertainties of the modelled values are given by the shaded lines.

median average deviation is used. For the modeled  $foF_2$  values, the uncertainties are calculated by propagating the errors of the different coefficients and parameters in the polynomial model and for the spectral model the uncertainty is calculated from the remaining terms in the Fourier transformation plus the error propagation (for the phases and amplitudes) whose dependence is modeled by polynomials. In Figs. 5 and 6 the uncertainties are given by solid bands.

The calculated  $foF_2$  by the polynomial model are plotted in Figs. 5 and 6 at noon (12:00) and at midnight (00:00) UTC time. At a first glance, qualitatively, both models describe well the seasonal and the solar cycle variations of  $foF_2$ . An important quality of both models is the ability to describe the fine structure in the annual variations of  $foF_2$  (e.g., 1996, 1997, 2006, and 2007). This applies more for the spectral model rather than for the polynomial. In result, the former model does a better job in fitting these values.

## 4.2 Comparison with IRI

For comparison, the values calculated by the International Reference Ionosphere (IRI2012) are plotted in Figs. 5 and 6. The figures show clearly that the fine structure (during the minima) of the  $foF_2$  cannot be reproduced by IRI2012 which gives an important advantage to the local modeling. The main divergences of the IRI2012 values are for low solar activity, where the local values of the critical frequency have a local maximum (in 1996, 1997, 2006 and 2007; in Figs. 5 and 6). It cannot be expected that a global model will produce the fine structure of a particular location which is one of the principal reasons for the development of a local model for every station.

The quantitative evaluation of the two models and the IRI2012 is made by evaluation of the differences between the modeled  $foF_2$  and the monthly median measured value. The distribution of these differences is plotted as a histogram in several cases. The evaluation of the different values is made by the standard deviations of the distributions. The results are given in Table 1.

Table 1

Standard deviation and skewness  
calculated for the polynomial and the spectral models and for the IRI2012

| Conditions | Polynomial | Spectral   | IRI2012   |
|------------|------------|------------|-----------|
| total      | 0.41/−0.35 | 0.47/−0.34 | 0.98/1.86 |
| nighttime  | 0.24/−0.65 | 0.34/−0.56 | –         |
| daytime    | 0.66/0.01  | 0.69/−0.05 | –         |
| solar max. | 0.55/−0.87 | 0.62/−0.76 | –         |
| solar min. | 0.22/2.71  | 0.25/2.37  | –         |

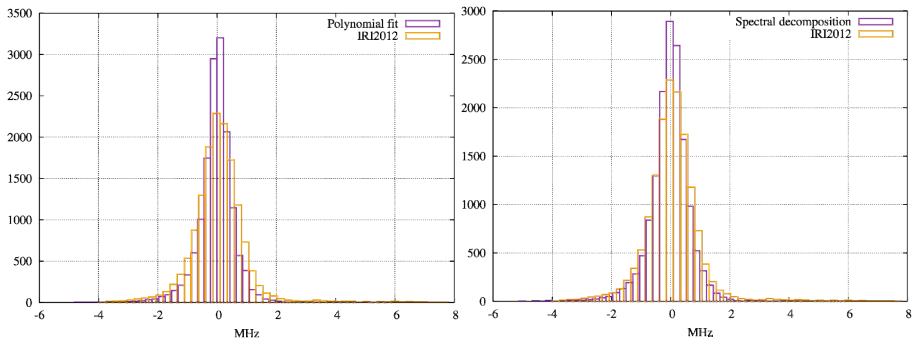


Fig. 7. Deviation between the measured and the modeled  $foF_2$  by the polynomial fitting and the spectral decomposition methods during the entire tracking period 1957-2010.

Several different “conditions” are compared: the entire data consisting of the  $foF_2$  calculated for every month and hour (that is the hourly monthly median); nighttime and daytime (using the data during the night hours and the day hours); and comparison during solar maximum and solar minimum.

The distribution of the total deviations (the difference between the modeled and measured  $foF_2$  medians) for the entire data is plotted in Fig. 7. While the deviations for both models are comparable, the deviations of the values obtained from IRI2012 show a larger spread and a large positive skewness (that is, the distribution of the values show a tail in the positive direction of the abscissa). Regarding the calculation of the deviations, it is shown that IRI2012 underestimates the measured values of the  $foF_2$ . The comparison between the spectral and the polynomial models gives a slight favor to the latter, for which the spread of the deviations from the measured values is slightly lower (see Table 1). Both models show the same trend when looking at the skewness – they are giving slightly larger deviations than the measured values for  $foF_2$ . When compared to the IRI2012 values, both local models produce about twice better values for the  $foF_2$ .

The histograms of the differences between the calculated and the measured monthly medians for the diurnal variations are plotted in Fig. 8. Both models yield comparable deviations from the measured monthly median. However, the polynomial model fits again better the values of the  $foF_2$  during daytime and nighttime conditions (Table 1). This applies especially for the nighttime data where the deviations from the measured values are much better when calculated from the polynomial model. Despite this, the spectral model has a better symmetry and consistency with a significantly smaller skewness. This will reduce the occasional large deviations during modeling of the  $foF_2$ . With regard to the diurnal behaviour, the performance of the two modeling approaches was examined during high and low solar activity.

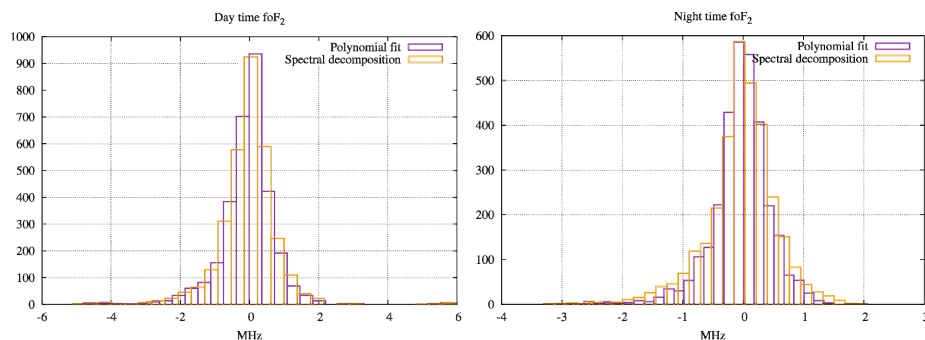


Fig. 8. Deviation between the measured and the modeled  $foF_2$  by the polynomial fitting and the spectral decomposition methods during day- and nighttime for the entire period between 1957 and 2010.

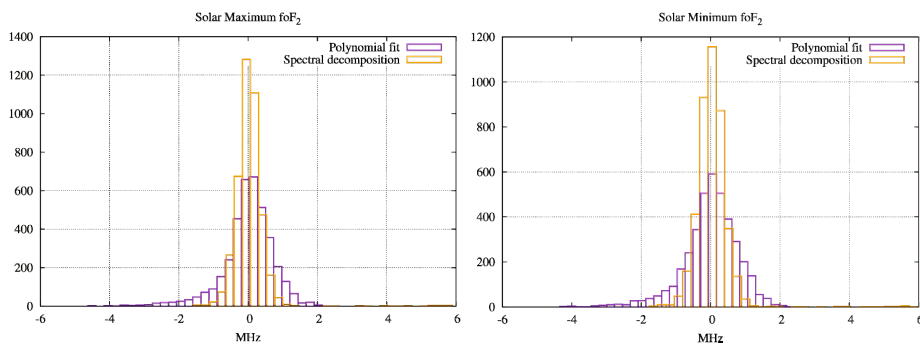


Fig. 9. Deviation between the measured and the modeled  $foF_2$  by the polynomial fitting and the spectral decomposition models during solar maximum and solar minimum for the entire period between 1957 and 2010.

The values of the deviations from the measured monthly medians for both models are plotted in Fig. 9. Under high and low solar activity, the deviations from the measured values for the spectral model are lower than those for the polynomial model. This can be attributed to the intrinsic periodicity in the spectral model which allows better fitting and reproduction of periodic dependencies. This was also observed in the description of the fine structure of the seasonal dependence where the spectral model fits better the measured data. These observations are supported by the standard deviations of the differences from the measured values, as reported in Table 1.

## 5. CONCLUSIONS

Local monthly median models for  $foF_2$  at Dourbes, Belgium, produce a better estimation of the  $F$ -layer critical frequency than the International Reference Ionosphere (IRI2012). The models are easily implemented and offer

opportunities for expansion (including additional parameters) and update. Two approaches were investigated for fitting the  $F$ -layer critical frequency as a function of the  $F_{10.7}$ : a polynomial fitting model using first and second-degree polynomials to model the available measured monthly median models. This model uses a large number of parameters and in general produces a better fitting for the entire dataset of hourly monthly median values. The second method reported in the work was to use spectral decomposition of the available data and express it as a sum of harmonics using a Fourier transformation. The resulting values calculated with this spectral model are having a slightly larger deviation from the calculated values by the polynomial model, but the deviations have a better symmetry (*i.e.*, better centered about the measured values). The intrinsic periodicity of this model allows it to better handle some small (fine) variations in the solar cycle and annual dependence of the monthly median  $foF_2$ . The general conclusion that can be drawn from this work is that the spectral decomposition has to be used as a basis for creating models of the  $F$ -layer critical frequency  $foF_2$ . Subsequently, further elaboration can be carried out for improvement of the calculated value by adding other geomagnetic or solar indices/parameters.

**Acknowledgments.** This work is funded by the Royal Meteorological Institute of Belgium (RMI) via the Belgian Solar-Terrestrial Center of Excellence (STCE). The solar activity index has been obtained from the US National Geophysical Data Center. The complete data-set used for this work can be obtained from the corresponding author.

## References

- Bilitza, D. (2001), International Reference Ionosphere 2000, *Radio Sci.* **36**, 2, 261-275, DOI: 10.1029/2000RS002432.
- De Franceschi, G., and A. De Santis (1994), PASHA: regional long-term predictions of ionospheric parameters by ASHA, *Ann. Geophys.* **37**, 2, 209-220, DOI: 10.4401/ag-4228.
- Fox, M.W., and L.F. McNamara (1988), Improved world-wide maps of monthly median  $foF_2$ , *J. Atmos. Terr. Phys.* **50**, 12, 1077-1086, DOI: 10.1016/0021-9169(88)90096-7.
- IRI (2012), The International Reference Ionosphere project, <http://irimodel.org/>.
- Jodogne, J.C., and S.M. Stankov (2002), Ionosphere-plasmasphere response to geomagnetic storms studied with the RMI-Dourbes comprehensive database, *Ann. Geophys.* **45**, 5, 629-647, DOI: 10.4401/ag-3529.

- Liu, L., W. Wan, and B. Ning (2004), Statistical modeling of ionospheric foF2 over Wuhan, *Radio Sci.* **39**, 2, DOI: 10.1029/2003RS003005.
- Mikhailov, A.V., V.V. Mikhailov, and M.G. Skoblin (1996), Monthly median foF2 and M(3000)F2 ionospheric model over Europe, *Ann. Geophys.* **39**, 4, DOI: 10.4401/ag-4019.
- Montgomery, D.C., C.L. Jennings, and M. KulaHCI (2008), *Introduction to Time Series Analysis and Forecasting*, Wiley, New York.
- Moraitis, G., Z. Kecic, and L. Cander (1991), Ionospheric modelling at single stations. **In:** *Proc. III PRIME Workshop, 21-25 January 1991, Rome, Italy*, 154-160.
- Muhtarov, P., and I. Kutiev (1998), Geomagnetically correlated statistical model (GCSM) for short-term prediction of ionospheric parameters. **In:** *Proc. 2nd COST251 Workshop "Algorithms and Models for COST251 Final Product", 30-31 March 1998, Side, Turkey*, 246-251.
- Muhtarov, P., I. Kutiev, L.R. Cander, B. Zolesi, G. de Franceschi, M. Levy, and M. Dick (2001), European ionospheric forecast and mapping, *Phys. Chem. Earth C* **26**, 5, 347-351, DOI: 10.1016/S1464-1917(01)00011-3.
- Pancheva, D.V., and P.Y. Mukhtarov (1996), A single-station spectral model of the monthly median F-region critical frequency, *Ann. Geophys.* **39**, 4, 807-818, DOI: 10.4401/ag-4020.
- Stamper, R., A. Belehaki, D. Buresová, L.R. Cander, I. Kutiev, M. Pietrella, I. Stanisławska, S. Stankov, I. Tsgouri, and Y.K. Tulunay (2004), Nowcasting, forecasting and warning for ionospheric propagation: tools and methods, *Ann. Geophys.* **47**, 2-3 Suppl., 957-983, DOI: 10.4401/ag-3281.
- Stanisławska, I. (1994), A single-station prediction model as a contribution to instantaneous mapping, *Ann. Geophys.* **37**, 2, 153-157, DOI: 10.4401/ag-4222.
- Stankov, S.M., J.-C. Jodogne, I. Kutiev, K. Stegen, and R. Warnant (2012), Evaluation of automatic ionogram scaling for use in real-time ionospheric density profile specification: Dourbes DGS-256/ARTIST-4 performance, *Ann. Geophys.* **55**, 2, 283-291, DOI: 10.4401/ag-4976.
- Xu, T., Z. Wu, J. Wu, G. Wei, and J. Feng (2008), A single-station spectral model of the monthly median foF2 over Chongqing, China, *Ann. Geophys.* **51**, 4, 609-618, DOI: 10.4401/ag-3022.
- Zolesi, B., L.R. Cander, and G. De Franceschi (1993), Simplified ionospheric regional model for telecommunication applications, *Radio Sci.* **28**, 4, 603-612, DOI: 10.1029/93RS00276.

Received 5 December 2014

Received in revised form 9 February 2015

Accepted 22 April 2015